JOURNAL OF VIROLOGY, Mar. 1995, p. 1699–1713 Vol. 69, No. 3
0022-538X/95/$04.00+0

Highly Specific Antibody to Rous Sarcoma Virus *src* Gene Product Recognizes Nuclear and Nucleolar Antigens in Human Cells

THÉRÈSE DAVID-PFEUTY* AND YOLANDE NOUVIAN-DOOGHE

Section de Biologie, Institut Curie, Centre Universitaire, 91405 Orsay Cedex, France

Received 19 July 1994/Accepted 7 December 1994

An antiserum to the Rous sarcoma virus-transforming protein pp60$^{v\text{-}src}$, raised in rabbits immunized with the bacterially produced protein αp60 serum (M. D. Resh and R. L. Erikson, J. Cell Biol. 100:409–417, 1985) previously reported to detect very specifically a novel population of pp60$^{v\text{-}src}$ and pp60$^{c\text{-}src}$ molecules associated with juxtareticular nuclear membranes in normal and Rous sarcoma virus-infected cells of avian and mammalian origin, was used here to investigate by immunofluorescence microscopy localization patterns of Src molecules in human cell lines, either normal or derived from spontaneous tumors. We found that the αp60 serum reveals nuclear and nucleolar concentrations of antigens in all the human cell lines tested and in two rat and mouse hepatoma cell lines derived from adult tumorous tissues but not in any established rat and mouse cell lines either untransformed or transformed by the *src* and *ras* oncogenes. Both the nuclear and nucleolar stainings can be totally extinguished by preincubation of the serum with highly purified chicken c-Src. We show also that the partitioning of the αp60-reactive proteins among the whole nucleus and the nucleolus depends mostly on two different parameters: the position in the cell cycle and the degree of cell confluency. Our observations raise the attractive possibility that, in differentiated cells, pp60$^{c\text{-}src}$ and related proteins might be involved not only in mediating the transduction of mitogenic signals at the plasma membrane level but also in controlling progression through the cell cycle and entry in mitosis by interacting with cell division cycle regulatory components at the nuclear level.

The c-*src* proto-oncogene, homolog of the viral *src* (v-*src*) oncogene responsible for the transforming activity of Rous sarcoma virus, has been highly conserved structurally throughout the evolution, being present and expressed in multicellular animals ranging from the most primitive ones, the sponges (6), to the highest vertebrates (46). However, no sequences homologous to that of *src* have been detected in the DNA from unicellular organisms, either *Escherichia coli* or yeasts. pp60$^{c\text{-}src}$ and related kinases belong to the family of nonreceptor protein tyrosine kinases. Specific mutations that affect their inherent kinase activity generally confer to these enzymes a transforming capacity (10, 23, 35), suggesting that they might normally participate in signalling pathways in charge of regulating cellular growth and proliferation. In addition, pp60$^{c\text{-}src}$ appears to be transiently activated during mitosis (8), perhaps as an indirect consequence of phosphorylation by p34^{cdc2} or related kinase (2, 24, 30, 45), which raises the possibility that c-Src may also exert special functions in this phase of the cell cycle. It is noteworthy then that pp60$^{c\text{-}src}$ usually exhibits a low level of expression in actively dividing cells but significantly higher levels in terminally differentiated cells such as neurons (11) and platelets (20, 39), providing a hint that pp60$^{c\text{-}src}$ could also participate in physiological events unrelated to growth and cell division. But, there is no real incompatibility in the fact that c-Src appears to serve in signalling pathways adapted to proliferating as well as to differentiated cells since, in both systems, high levels of pp60$^{c\text{-}src}$ have been detected in apparent association with intracellular vesicles such as the chromaffin granules in chromaffin cells (21, 36), the synaptic vesicles in neurons (5, 26), and endocytotic vesicles in fibroblasts (13, 25). This type of vesicular structures has been implicated in the transport of material between different subcellular compartments, in particular of growth factor-growth factor receptor complexes from the plasma membrane to the centrosomal area in dividing cells, as well as in exocytosis in specialized secretory cells. These observations suggest that pp60$^{c\text{-}src}$ could generally be involved in controlling intracellular traffic of proteins as well as traffic in and out of the cell and/or in regulating functions in which these intracellular transport vesicles also participate.

Recently, we have shown that myristoylation-defective (Myr$^-$) c-Src proteins do not simply lose the ability to bind with a high affinity to plasma membrane-associated receptors (19, 40, 42) but that they also acquire the ability to translocate inside the nucleus, in particular during an artificial growth arrest induced by cell cycle-blocking agents or by serum deprivation and also during the G_2 phase of a normal cell cycle, and to associate strongly with components of the spindle apparatus and of the interchromosomal space during mitosis (12). This finding was consistent with the results of other studies that reported either the occurrence of a c-Src translocation into the nucleus in response to in vitro calcium-induced keratinocyte differentiation (47) or a nuclear location of a c-Fgr variant in myeloid cells and in stably transfected fibroblasts, all supporting the notion that members of the Src family, apparently under specific conditions, may achieve a conformational state favorable to nuclear targetting.

The report of Zhao et al. (47) was of particular interest since it raised the possibility that the conditions that permit a stable nuclear c-Src expression might be fulfilled in differentiated cells. In contrast to rat and mouse embryonic tissues, human tissues are difficult to establish in culture, but numerous established human cell lines have been derived from tumorous adult tissues. Interestingly, certain tumor-derived cell lines have been reported to have the tendency to lose their tumorigenic

* Corresponding author. Mailing address: Section de Biologie, Institut Curie, Centre Universitaire, Bâtiment 110, 91405 Orsay Cedex, France. Phone: 69 86 30 75. Fax: 69 07 45 25.

TABLE 1. Status of p53 gene in various tumor-derived human cell lines analyzed

Tumor cell line	Tumor type	Polymorphism at codon 72	No. of 17p alleles	Codon	Mutation nucleotide	Amino acid nucleotide	Reference
KHOS-240	Osteosarcoma	Arg	1	156	CGC→CCC	Arg→Pro	44
T-47D	Breast carcinoma	Pro	1	194	CTT→TTT	Leu→Phe	31
A-431	Epidermoic carcinoma	Pro	1	273	CGT→CAT	Arg→His	9
MCF-7	Breast carcinoma	Pro/Arg	2	None	None	None	7
HeLa	Epitheloid cervix carcinoma	Pro/Arg	2	None	None	None	28

properties and to reexpress characteristics of differentiated cells following long-term ex vivo culturing, indicating that although they have reacquired the capacity to grow and divide, in contrast with normal differentiated tissue cells, tumor cell lines may still possess features belonging naturally to the differentiated state. We thought that such tumor-derived cell lines issued from adult tissues might be an appropriate material in which to search for a nuclear subset of Src molecules. We then looked for the intracellular distribution of anti-pp60^{src}-reactive proteins in human tumor-derived cell lines, using three different anti-Src antibodies: two mouse monoclonal antibodies MAbs 327 (27) and GD11 (37) and a polyclonal antibody raised in rabbit (αp60 [41]). Whereas the two anti-Src MAbs detected human Src populations similar to those previously described in established mouse and rat cell lines, the αp60 serum revealed nuclear and nucleolar concentrations of antigens in all the human tumor cells assayed as well as in the untransformed human WI-38 cell line. A similar nuclear anti-pp60^{src}-reactive protein population has also been detected in two established hepatoma cell lines derived from adult rat and mouse tumors, but it has never been observed in any established rat and mouse cell lines either untransformed or transformed by the *src* and *ras* oncogenes. This finding confirms and extends the few previous accounts of the presence of c-Src or c-Src-related proteins in the nucleus.

MATERIALS AND METHODS

Cell lines. The cell lines KHOS-240, T47-D, A-431, MCF-7, and HeLa were kindly provided by Evelyne May. The status of the p53 gene and the origin of the various human transformed cell lines are presented in Table 1. The untransformed WI-38 line was obtained from the American Type Culture Collection. Cells were all grown in Dulbecco's modified Eagle's medium supplemented with 10% fetal bovine serum and antibiotics and maintained in a 10% CO_2 humidified atmosphere. Plasmid-transfected NIH 3T3 cells that overexpress wild-type [NIH(pMc-Src/focus)B] and nonmyristoylated [NIH(pcLN/pSV$_2$neo/MC)C] chicken c-Src have been previously described (12, 22) and were kindly provided by David Shalloway.

Cell culture and synchronization. Cells were cultured in 35-mm-diameter dishes on 22-mm^2 coverslips in Dulbecco's modified Eagle's medium containing 5% fetal bovine serum and antibiotics in 10% CO_2, at 37°C for at least 2 days before immunofluorescence observation. The average cell density in standard experiments was 10^4 cells cm^{-2}. When cultures enriched in premitotic and mitotic cells were to be examined, synchronization at the G_1-S boundary was first effected by a thymidine-aphidicolin double block: cells were grown in normal medium for 2 days and then sequentially incubated with 2.5 mM thymidine (16 h), normal medium (8 h), and 5 μg of aphidicolin (16 h) per ml. Immunofluorescence with anti-tubulin antibody and DAPI (4′, 6-diamidino-2-phenylindole) showed that mitotic cells were most prevalent 8 to 12 h after the release from the double block, depending on the particular cell line.

Antibodies and reagents. (i) Procedure for immunofluorescence. Anti-p60 polyclonal rabbit antiserum, αp60 (41), and mouse anti-Src MAb GD11 (37) were generous gifts from Marilyn Resh and Sarah Parsons, respectively. Mouse anti-Src MAb 327 (27) was purchased from Clinisciences (Paris, France), and rat anti-tubulin MAb YOL1/34 was purchased from Biosys (Compiègne, France). The mouse anti-cyclin B1 MAb, GNS11, directed against an epitope located between amino acids 21 and 88 from human cyclin B1, was generously provided by Steven Shiff (Ed Harlow's Laboratory). DNA was counterstained with 1 μg of DAPI fluorescent dye (Sigma, St Quentin Fallairet, France). The purified chicken c-Src protein utilized in the competition experiments was prepared by Mossaad Abdel-Ghany and Bel Hilton (David Shalloway's Laboratory) according to the procedure elaborated by Zhang et al. (48); this procedure essentially makes use of two affinity columns prepared with copolymers containing glutamate and tyrosine (4:1; poly-E_4Y_1) and glutamate, alanine, and tyrosine (6:3:1; poly-$E_6A_3Y_1$) to obtain highly purified (95%) and enzymatically stable preparations of c-Src and v-Src kinase starting from Triton X-100 extracts of insect cells infected with *Autographa california* baculovirus into which the c-Src- or v-Src-coding sequences had been recombined. The protein concentration needed to extinguish almost totally the αp60 immunostaining (serum dilution, 1:1,500) in all cell lines, or the MAb 327 staining (5 μg/ml) in NIH 3T3 c-Src-overexpresser cells, was 15 μg/ml.

Secondary antibodies (Interchim or Institut Pasteur, Montluçon and Marnes la Coquette, France) were goat immunoglobulin G (IgG) Fab fragments from antibodies directed against either mouse, rat, or rabbit IgG. (The goat anti-rat IgG was preabsorbed against a mouse column to eliminate cross-reactivity; a reciprocal preabsorption was used for the goat anti-mouse IgG.) These fragments were conjugated with either fluorescein isothiocyanate or tetramethyl rhodamine isothiocyanate. These secondary antibodies gave essentially undetectable background fluorescence.

Single- or double-fluorescent cell labeling was done described previously (14) following fixation with 3% paraformaldehyde and subsequent permeabilization by a short treatment (4 min) with 0.1% Triton X-100 at room temperature. Alternatively, fixation was carried out by treatment with methanol at −20°C for 6 min. The second procedure, however, should be utilized with caution, mainly if one is looking for proteins supposedly interacting with membrane-associated structures. Indeed, observation by phase-contrast microscopy indicated that such treatment greatly alters the plasma and intracellular membrane architectures by creating large holes in them. Fluorescence microscopy was performed with a Leitz microscope equipped with fluorescein, rhodamine, and DAPI filters and a 40× oil objective. Photographs were taken with Kodak TMax 400 film.

Immunoprecipitation and immunoblotting. Cellular extracts for immunoprecipitation and immunoblotting were prepared in RIPA buffer containing 10 mM Tris (pH 7.2), 0.15 M NaCl, 1% sodium deoxycholate, 1% Triton X-100, 0.1% sodium dodecyl sulfate (SDS), and 100 kallikrein inactivator units of aprotinin. For immunoprecipitation, the clarified supernatants were incubated with the mouse MAb or rabbit polyclonal antibody of interest, and the antigen-antibody complexes were collected on beads of protein G- or protein A-Sepharose, respectively. The separation of the proteins present in the cellular extracts or in the immunoprecipitates was effected on SDS–8.5% polyacrylamide gels after the samples were boiled for 3 min in sample buffer. Immunoprecipitation of [^{35}S]methionine-labeled cellular extracts was done with subconfluent cell cultures that had been preincubated for 1 h in methionine-free medium before they were radiolabeled with 100 μCi of [^{35}S]methionine (>77%) and [^{35}S]cysteine (>18%) protein-labeling mix (>100 Ci/mmol; New England Nuclear) per ml for 24 h in the appropriate medium. For immunoblotting, the fractionated proteins were transferred to nitrocellulose overnight at 20 V and, after blocking, probed in the presence of the antigen with the appropriate antibody solution following overnight incubation at 4°C. After several washes, the filters were incubated with horseradish peroxidase-conjugated antibody, and detection of the immune complex was done by using the ECL (Amersham, France) Western immunoblotting system.

RESULTS

αp60 serum and immunoprecipitation of 60-kDa protein in normal and transformed human cell lines with various anti-Src antibodies. The properties of the αp60 serum have been described in some detail previously by Resh and Erickson (41). They showed that the high-titer αp60-specific antisera obtained by immunizing rabbits with p60$^{v\text{-}src}$ expressed in *E. coli* (17) are highly specific for the amino-terminal portion of pp60$^{v\text{-}src}$ and recognize a subclass of v-Src and c-Src molecules not revealed by tumor-bearing rabbit sera. On the other hand, cell fractionation experiments indicated that these αp60-reactive Src populations were more specifically distributed inside P1 nuclear fractions of cell lysates, and immunofluorescence

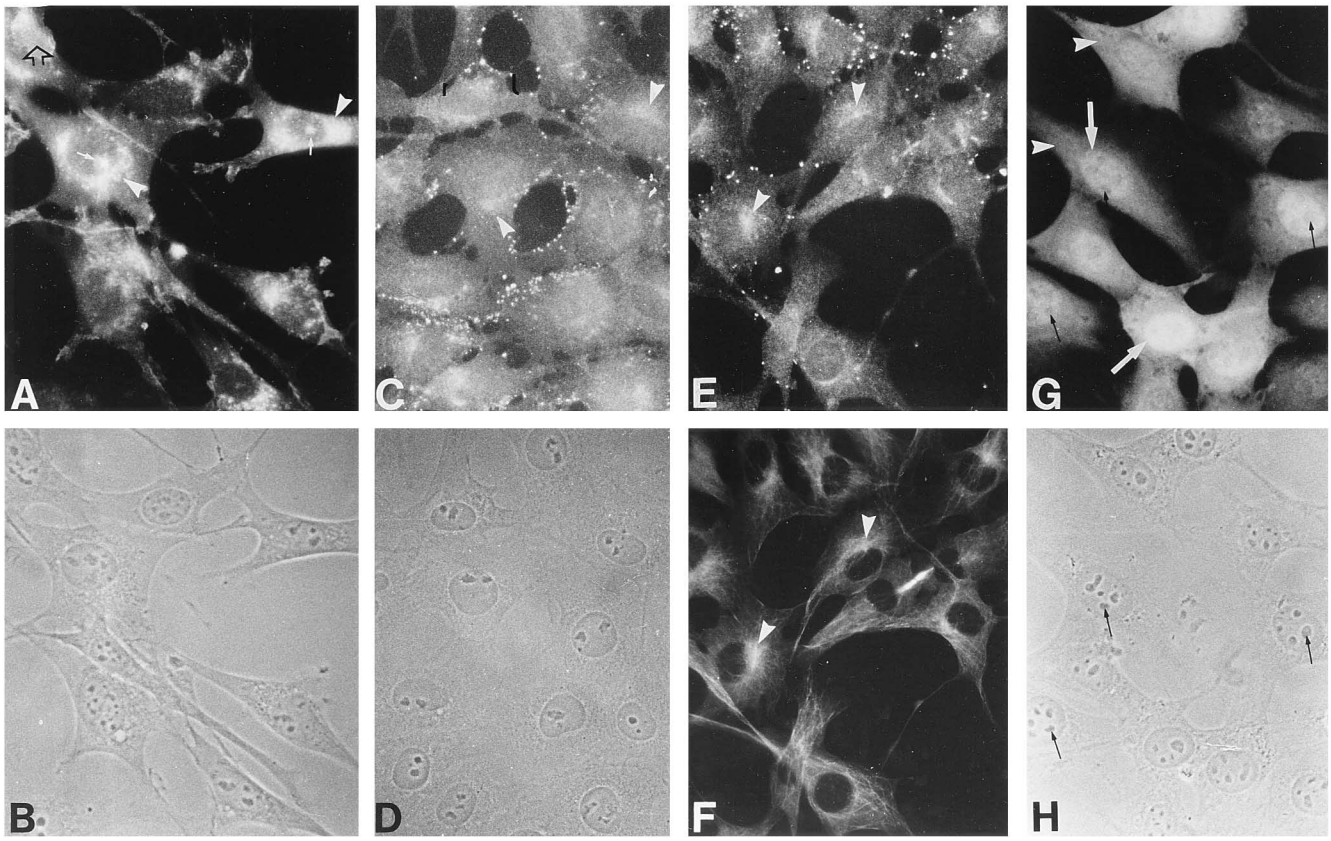

FIG. 1. Immunolabeling with αp60 serum (A, C, E, and G) and corresponding phase-contrast images (B, D, and H) or anti-tubulin staining (F) of mouse and rat cells. The cell lines displayed are NIH (pMc-Src/focus)B (A and B), which overexpresses a normal chicken c-Src protein; Rat-1 (C to F); and NIH(pcLN/pSV$_2$neo/MC)C, which overexpresses a nonmyristoylated c-Src protein and was observed following a thymidine-aphidicolin double block (G and H). The αp60 serum clearly exhibits the same staining patterns as MAb 327 in the NIH 3T3 cells overexpressing either normal or Myr$^-$ c-Src proteins. (A) Interaction with centrosome (tiny arrows), perinuclear vesicles (arrowheads), and plasma membrane (open arrow) in the NIH(pMc-Src/focus)B line; (G and H) labeling of cytoplasm (arrowheads), nucleus (large arrows), and, to a lesser extent, nucleolus (tiny arrows) in Myr$^-$ c-Src-overexpresser cells. In the Rat-1 cells, the αp60 serum also clearly detected perinuclear concentrations of c-Src (arrowheads in panels C and E) that accumulate in the centrosomal area (arrowheads in panel F).

studies revealed a distinct pattern of perinuclear fluorescence for pp60$^{v\text{-}src}$ in Rous sarcoma virus-infected chicken embryo fibroblasts. But no immunofluorescence staining for pp60$^{c\text{-}src}$ in mammalian cells was carried out in these earlier studies. More recently, we have shown that the αp60 serum generated the same immunofluorescence patterns as those exhibited by the two anti-Src MAbs, 327 and GD11, in NIH 3T3 cells overexpressing either a normal or a myristoylation-defective c-Src protein (12, 13) (Fig. 1A and G, respectively). Briefly, in the NIH 3T3 c-Src-overexpresser cells, the αp60 antibodies concentrate on three main subcellular sites: the plasma membrane (Fig. 1A, open arrow) the centriolar areas (Fig. 1A, tiny arrows), and a cluster of patches surrounding the nuclei (Fig. 1A, arrowheads). In the NIH 3T3 Myr$^-$ c-Src-overexpresser cells, this serum also reveals the two major Myr$^-$ c-Src partitionings among the cytoplasm (Fig. 1G, arrowheads) and the nucleus (Fig. 1G, arrows), the latter distribution being greatly enhanced following a thymidine-aphidicolin double block; the nuclear staining is somewhat less intense in the nucleolar regions (Fig. 1G and H, tiny arrows). In the established mouse NIH 3T3 and rat cell lines (FR3T3 and Rat-1), the αp60 serum detects a discreet juxtanuclear concentration of the endogeneous pp60$^{c\text{-}src}$ (shown in the Rat-1 cell line) (Fig. 1C and E, arrowheads); this location coincides with the centrosomal area in which the interphasic microtubules are converging (Fig. 1E and F, arrowheads).

The αp60 serum had not been previously assayed in human systems in contrast with anti-Src MAbs 327 and GD11, which have previously been reported to readily and specifically immunoprecipitate enzymatically active pp60$^{c\text{-}src}$ from extracts of uninfected human fibroblasts for GD11 and of normal as well as transformed human epidermoid cells for both antibodies (47). These two MAbs immunoprecipitate detectable amounts of human pp60$^{c\text{-}src}$ in a normal, untransformed WI-38 cell line and in five tumor-derived cell lines, HeLa, KHOS-240, MCF-7, T47-D, and A-431 (shown for GD11 in Fig. 2, lanes 2). Figure 2, lanes 1 and 3, show the patterns of [^{35}S]methionine-labeled proteins obtained following immunoprecipitation of equivalent amounts of radiolabeled cellular extracts with either a normal rabbit serum (lanes 1) or the αp60 serum (lanes 3). We observe that the αp60 serum also specifically reacts with a 60-kDa protein (migrating at the same level as the GD11-specific 60-kDa band) clearly visible in the HeLa, KHOS-240, and WI-38 cell lines but less readily detectable in the MCF-7, T47-D, and A-431 cell lines in which the amount of 60-kDa protein immunoprecipitated by αp60 is obviously much less than the amount of pp60$^{c\text{-}src}$ immunoprecipitated by GD11. (This may be accounted for by the fact that these latter cells tend to form bidimensional multicellular aggregates on the substratum in which the most compacted cells in the center of the aggregates tend to show a reduced level of accumulation of the αp60-reactive molecules in their nucleus.) The bands which appear

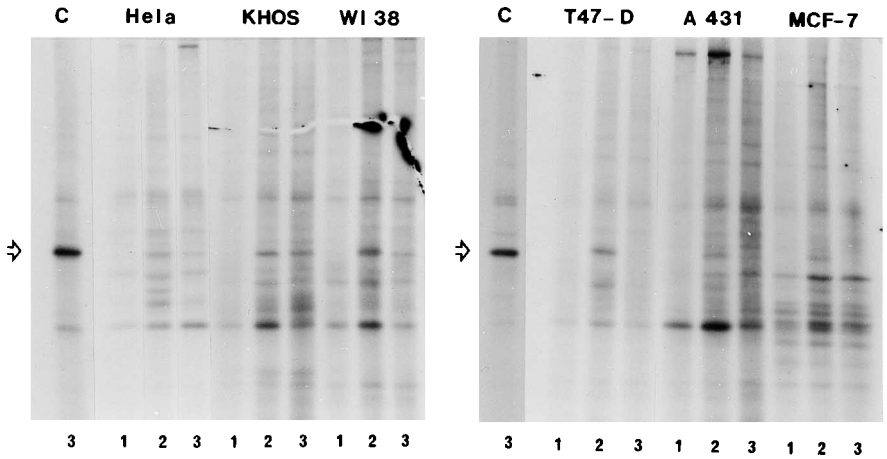

FIG. 2. Immunoprecipitation of [^{35}S]methionine-labeled human cells with anti-Src antibodies GD11 (lanes 2), αp60 (lanes 3), and normal rabbit serum (lanes 1). Immunoprecipitation of Myr$^-$ c-Src-overexpresser cells (lanes C) with αp60 serum was used as a control to position the 60-kDa immunoreactive bands on the gels (open arrows).

in lanes 1 correspond to unspecific absorption on the protein A-Sepharose matrix of [^{35}S]methionine-labeled proteins present in the cellular extracts. For comparison, lanes C exhibit the immunoprecipitation pattern with αp60 serum of [^{35}S]methionine-labeled NIH(pcLN/pSV$_2$neo/MC)C cellular extracts (these cells overexpress a nonmyristoylated c-Src protein up to a level 20-fold higher than the level of endogeneous mouse pp60$^{c\text{-}src}$). We further have verified that the 60-kDa protein specifically immunoprecipitated by the αp60 serum was likely to be related to c-Src by immunoblotting αp60 immunoprecipitates with MAb 327. We have shown that, indeed, MAb 327 detects a single 60-kDa band in αp60 immunoprecipitates of HeLa, KHOS-240, and WI-38 cells (Fig. 3).

Detection of various subpopulations of anti-pp60^{src} proteins in unsynchronized normal and transformed human cell lines by using different anti-Src antibodies. The six human cell lines examined can be categorized into two groups. Group A comprises the normal, untransformed WI-38 cell line and the two tumor-derived cell lines, HeLa and KHOS-240. These cells in culture remain well individualized at low plating densities and begin to contact each other only at high cell densities because of the lack of available spreading space on the substratum. In contrast, cells of group B (MCF-7, A-431, and T47-D) do not remain dispersed in culture, even at low cell densities, but on the substratum, they tend to form compact, bidimensional, multicellular aggregates from which mainly peripheral cells appear to actively grow and divide. Such a distinctive feature probably reflects the fact that these cells have the propensity to form strong intercellular contacts and that, after cell division, daughter cells will remain attached instead of separating and migrating on the substratum.

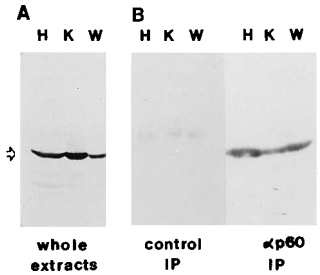

FIG. 3. Detection of 60-kDa protein (open arrow) in whole extracts (A) and αp60 immunoprecipitates (IP) of HeLa (lanes H), KHOS-240 (lanes K), and WI-38 (lanes W) cells (B) by immunoblotting with MAb 327. Normal rabbit serum immunoprecipitates were used as controls.

(i) Subcellular distribution of MAb 327- and GD11-immunoreactive proteins in human cells. Immunolabeling the human cells belonging to group A with MAbs 327 and GD11 gives weak, apparently unspecific fluorescence resembling that described for the mouse NIH 3T3 cell line (13), which concentrates in the central region of the cells over and around the nucleus (shown for MAb 327 in the HeLa cells [Fig. 4A] and for GD11 in the WI-38 cells [Fig. 4C]). With group B, the two anti-Src MAbs primarily intensely stain the cell-to-cell contact areas (Fig. 4E, G, K, M, and O, long, thin arrows). In addition, MAb GD11 concentrates on juxtanuclear structures, the most intense staining being observed in the A-431 cell line (Fig. 4E, I, K, M, and O, arrowheads). This GD11-specific staining of juxtanuclear structures was likely specific since it was extinguished by preincubation with purified c-Src (data not shown).

(ii) Subcellular distribution of αp60-immunoreactive protein in human cell lines. Considering the fact that the αp60 serum and the two anti-Src MAbs generate quite similar pp60^{src} distribution patterns in normal, established and Rous sarcoma virus-transformed rat and mouse cells, we were initially surprised to find that the αp60 antibodies very specifically recognize in human cells nuclear subpopulations of an Src protein which are not detected by either MAb 327 or GD11. This finding, illustrated in Fig. 4, has been made with different batches of anti-Src antisera from three different rabbits and the six different human cell lines analyzed. At first glance, it can be noted that the αp60-specific immunostaining (Fig. 5A, C, E, G, I, and K) distributes inside the nucleus among the nucleoli (Fig. 5, tiny arrows) and the whole nucleus (Fig. 5, large arrows) in various ratios from one cell line to another and from one cell to another inside the same cell population. Sometimes, among a population of cells exhibiting marked αp60 nuclear staining, a few isolated, negative cells can be observed (Fig. 5, curved arrows). This latter observation, together with the former observation that the ratio of nucleolar-to-nuclear αp60 staining varies from cell to cell within a given cell population, argues against the possibility of an artefactual, unspecific interaction between the αp60 antibodies and nuclear structures. Moreover, the αp60 serum interacted with juxtanuclear struc-

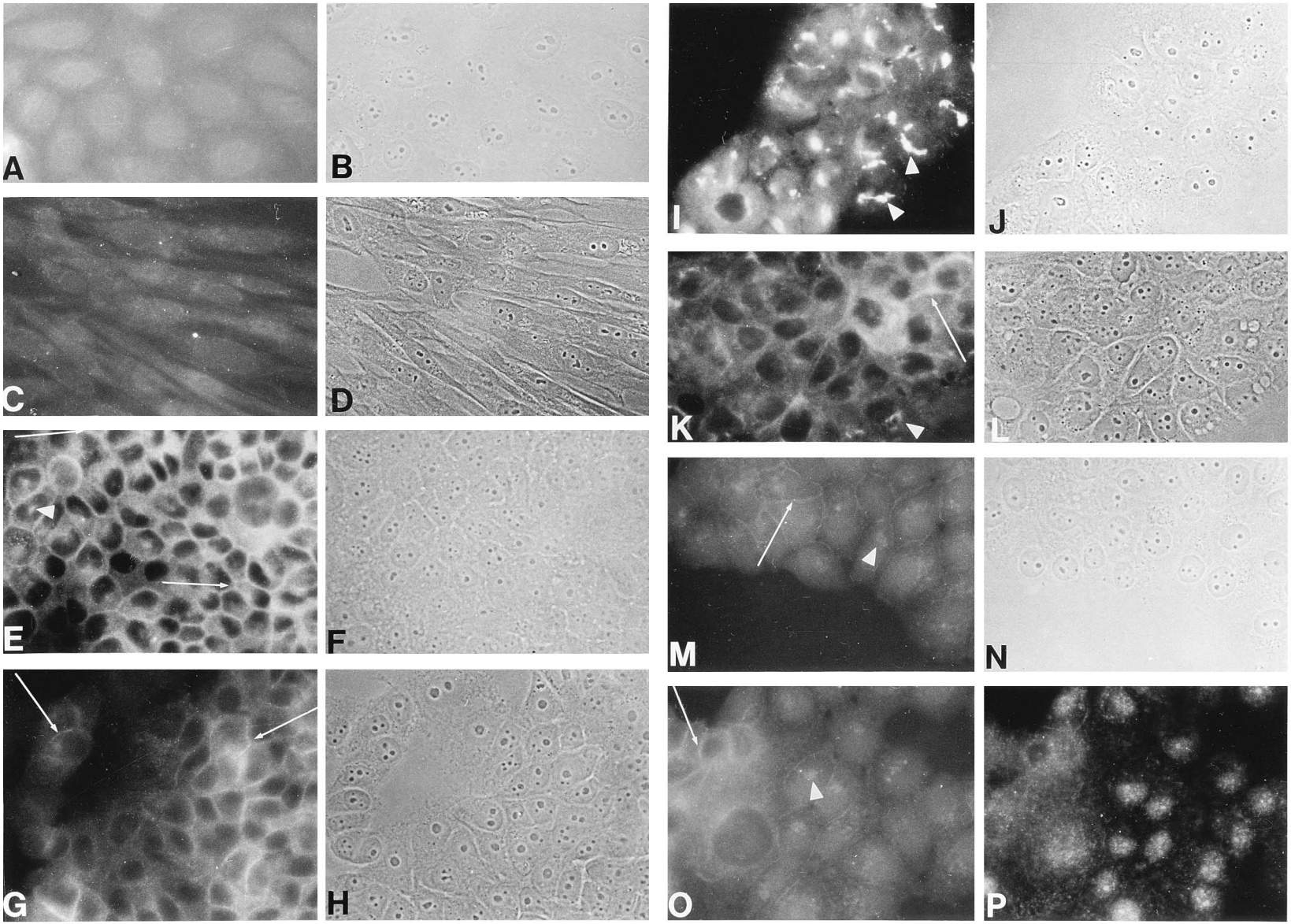

FIG. 4. Immunolabeling with MAb 327 (A and G) or GD11 (C, E, I, K, M, and O) and corresponding phase-contrast images (B, D, F, H, J, L, and N) or αp60 staining (P) of various human cells. The cell lines displayed are HeLa (A and B), WI-38 (C and D), MCF-7 (E to H), A-431 (I to L), and T47-D (M to P). The MAb 327 anti-Src antibody does not significantly reveal any particular structure in subconfluent cells whereas MAb GD11 clearly reveals a c-Src subpopulation associated with juxtanuclear material, strongly in the A-431 cell line (I and K, arrowheads) and more faintly in the MCF-7 and T47-D cell lines (E, M, and O, arrowheads). The two anti-Src MAbs concentrate at intercellular contact areas (E, G, K, M, and O, long arrows), more or less heavily depending of the cell line. In no instances was nuclear or nucleolar staining detected with the two anti-Src MAbs (compare the immunofluorescence and phase-contrast images).

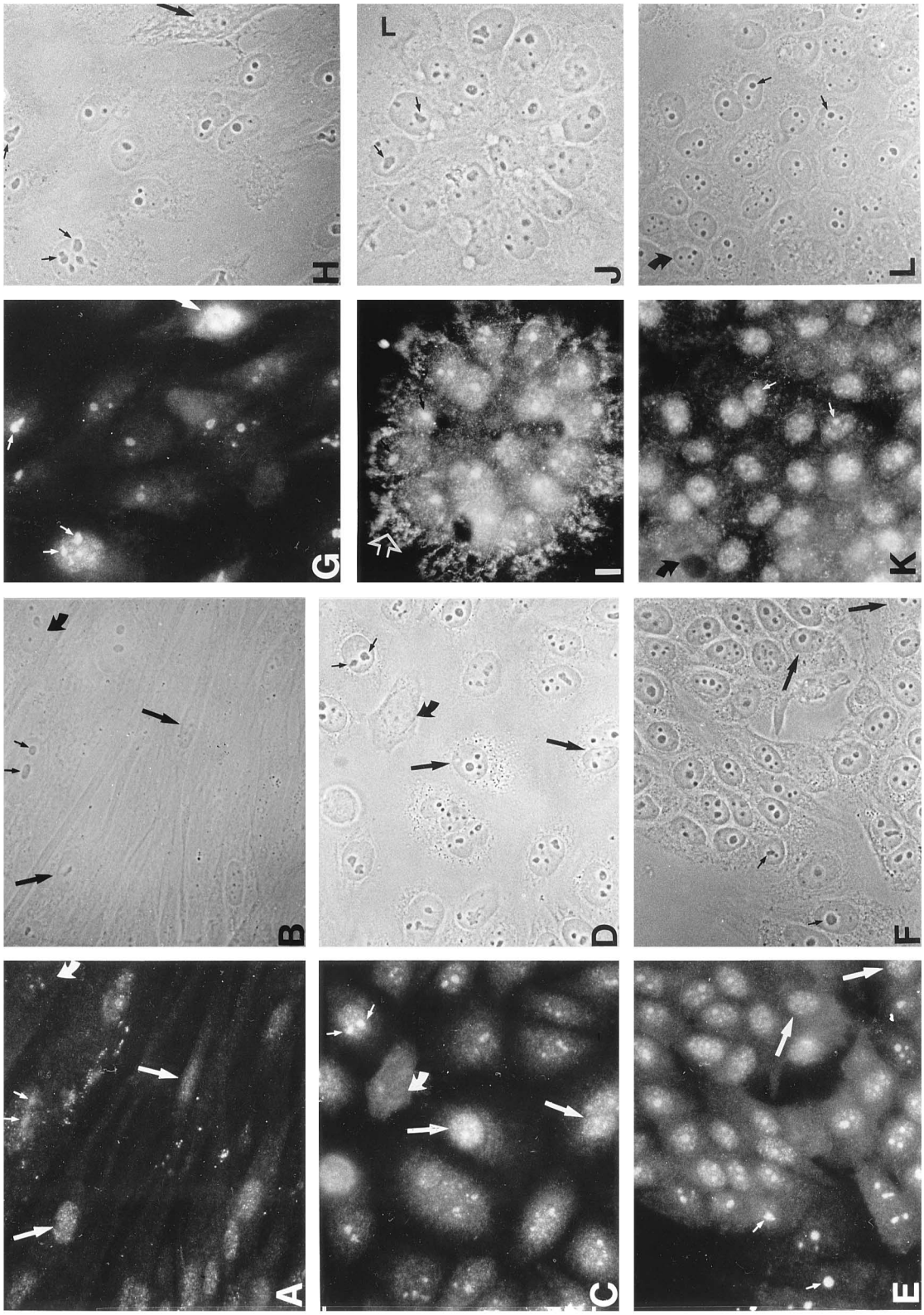

FIG. 5. Immunolabeling with αp60 serum (A, C, E, G, I, and K) and phase-contrast microscopy (B, D, F, H, J, and L) of various human cell lines. The cell lines displayed are WI-38 (A and B), HeLa (C and D), MCF-7 (E and F), KHOS-240 (G and H), A-431 (I and J), and T47-D (K and L). Individual cells exhibited various degrees of nuclear versus nucleolar staining with the αp60 serum. The tiny arrows point out a few nucleoli heavily labeled with the αp60 serum, and the larger arrows identify nuclei showing mostly nuclear staining despite the presence of well-formed nucleoli. The curved arrows (A, B, C, D, K, and L) point out a few unstained nuclei. In the A-431 cell line (I and J), the αp60 serum also very strongly labels juxtanuclear structures (I, open arrow).

tures, most obviously in the A-431 cell line (Fig. 5I, open arrow), like the MAb GD11. We have affinity purified the anti-Src antibodies present in αp60 serum by retroelution of the immunoglobulins bound to the bacterially expressed and purified chicken c-Src protein on a nitrocellulose sheet, according to the procedure described by Bailly et al. (4). This purified antibody still visibly immunoprecipitated a 60-kDa protein in the human cells from group A and clearly associated with nucleolar structures in the KHOS-240 cell line in which the whole serum also interacted primarily with the nucleoli (Fig. 5G). But, because of a higher level of background fluorescence (probably due to a partial denaturation of IgG during the purification procedure), the subtle variability during the cell cycle between the respective levels of nucleolar and nuclear staining observed with the whole αp60 serum could not be clearly distinguished. For that reason, all the pictures presented here were obtained with the whole serum utilized at a 1:1,500 dilution. Interestingly, nuclear αp60 immunostaining was also detected in three hepatoma cell lines derived from adult human, rat, and mouse tumors, although to various extents (the degree of intensity being highest in the human cells, intermediate in the rat ones, and low in the mouse system). But, it was undetectable in any established rat and mouse cell lines transformed either by the *src* or *ras* oncogene (data not shown).

To further assess the specificity of the interaction between the αp60-immunoreactive antigen and nuclear structures, immunostaining of the human cells was done with αp60 serum previously incubated in the presence of 7 μg of purified c-Src per ml. An almost quasi-total extinction of the αp60-specific nuclear staining was obtained under these conditions for all cell lines (Fig. 6D, I, and M). At this concentration of the c-Src protein, a faint residual nucleolar labeling can sometimes still be observed (Fig. 6D and I, tiny arrows). Immunolabeling of neither the microtubule network (Fig. 6E) nor nuclear cyclin A (data not shown) was blocked following the preincubation of anti-tubulin and anti-cyclin A antibodies with 7 μg of purified c-Src per ml. Doubling the concentration of purified c-Src permitted total elimination of the nuclear αp60-specific immunostaining (data not shown), without washing out a diffuse and punctate background fluorescence, such as that appearing in Fig. 6D, I, and M, and similar to that observed for normal rabbit serum in place of αp60.

The cell fields exhibited in Fig. 5 have been selected to represent, as closely as possible, whole-cell populations generated under standard plating and asynchronous growth conditions (see Materials and Methods). A quick look at the figures immediately reveals several gross features of the αp60 immunostaining in the different human cell lines. Firstly, the majority of tumor cells belonging to group B (which tend to form bidimensional multicellular aggregates on culture dishes) display the two nuclear αp60-specific staining patterns, the nucleolar one, which is generally the most intense, and the extranucleolar one, which concentrates into tiny dots that spread homogeneously throughout the whole nucleus. It can also be noted that the cells situated at the periphery of the multicellular aggregate representative of the MCF-7 cell line (Fig. 5E) exhibit mostly the nucleolar αp60 immunostaining and less detectable nuclear immunostaining, in contrast to the cells situated inside the aggregate. Among the three cell lines of group A (whose cells remain well dispersed at low or medium plating density), the normal, untransformed one (WI-38 [Fig. 5A]) presents an αp60 immunostaining pattern somewhat distinct from that presented by the two tumor-derived cell lines (HeLa [Fig. 5C] and KHOS-240 [Fig. 5G]), the nucleolar αp60 immunostaining being generally more prominent in the latter systems.

From these rough observations, we envisaged the following possibilities. (i) In the two human tumor-derived cell lines belonging to group A, the αp60-reactive antigens are segregated inside the nucleoli during the almost full length of the cell cycle; they become free to disperse inside the whole nucleus only during a short period of the cell cycle, presumably in G_2, at which time important changes in the nuclear organization must occur in order to prepare the next phase of chromosome condensation. (ii) The exclusion of the αp60-reactive proteins from the nucleoli and their dispersion through the whole nucleus could also be induced by cell-to-cell contact formation; this would explain the features of the αp60 immunostaining observed for the B group tumor cells.

To test our hypothesis, we sought possible changes in the immunolocalization patterns of the αp60-reactive proteins as a function of the cell cycle and of the degree of cell-to-cell aggregation in the HeLa and KHOS-240 cell lines.

Changes in immunolocalization patterns of αp60-immunoreactive proteins as a function of the cell cycle in HeLa and KHOS-240 cell lines. Attempts to arrest cell cycling in cultured human cancer cells by serum deprivation down to 0.5% for 3 days was apparently totally ineffective according to the following criteria. (i) The nuclear concentration of cyclin A following serum starvation was still observed at a rate (in about 50% of the cells but at a somewhat less extent in the HeLa cell line) almost similar to that observed in the control cells; we recall that in untransformed mammalian fibroblasts and HeLa cells, nuclear translocation of cyclin A has been shown to occur right before the G_1-S-phase transition (18, 38). (ii) According to the tubulin and DAPI staining, the percentage of cells undergoing mitosis in serum-starved cell populations was also equivalent (between 2 and 3%) to that detected in control cell populations.

Whereas serum deprivation was ineffective at arresting the human tumor cells in G_0, a thymidine-aphidicolin double block was apparently efficient in preventing cell progression through the G_1-S-phase boundary, since very few mitotic cells were observed before release from the double block but a large number of mitotic cells were obtained between 8 to 12 h following release depending of the particular cell line. Unexpectedly, however, at time zero following the double-block release, very intense αp60 immunostaining that spread over the whole nucleus (including the nucleolus) was observed in the quasi-total population of HeLa cells (Fig. 7A) and in 50 to 70% of the KHOS-240 cell population (Fig. 7E). Such behavior is reminiscent of that of the overexpressed Myr^- c-Src protein in NIH 3T3 cells following a similar treatment (12). Like that for the Myr^- c-Src protein also, the nuclear accumulation of αp60-reactive protein decreased as cells were released from the double block at later times and did not reappear at the following G_1-S-phase transition (between 20 to 24 h later), indicating that this effect can be attributed to an artefact and did not reflect a natural nuclear overexpression of the protein prior to entry into the S phase. Following the first round of mitosis after release from the thymidine-aphidicolin double block, that is, as the cells were reentering a new cell cycle, the αp60 staining in the HeLa and KHOS-240 cell lines did not differ significantly from that exhibited by unsynchronized cell populations. It was unchanged during the next complete G_1 and S phases, that is, between 11 and 30 h after the double-block release.

In exponentially growing HeLa cell populations, cyclin B1 has been shown to start accumulating in the cytoplasm at a significant level roughly at the S-G_2 border (4). Double immunolabeling with the αp60 antiserum and an anti-cyclin B1 MAb

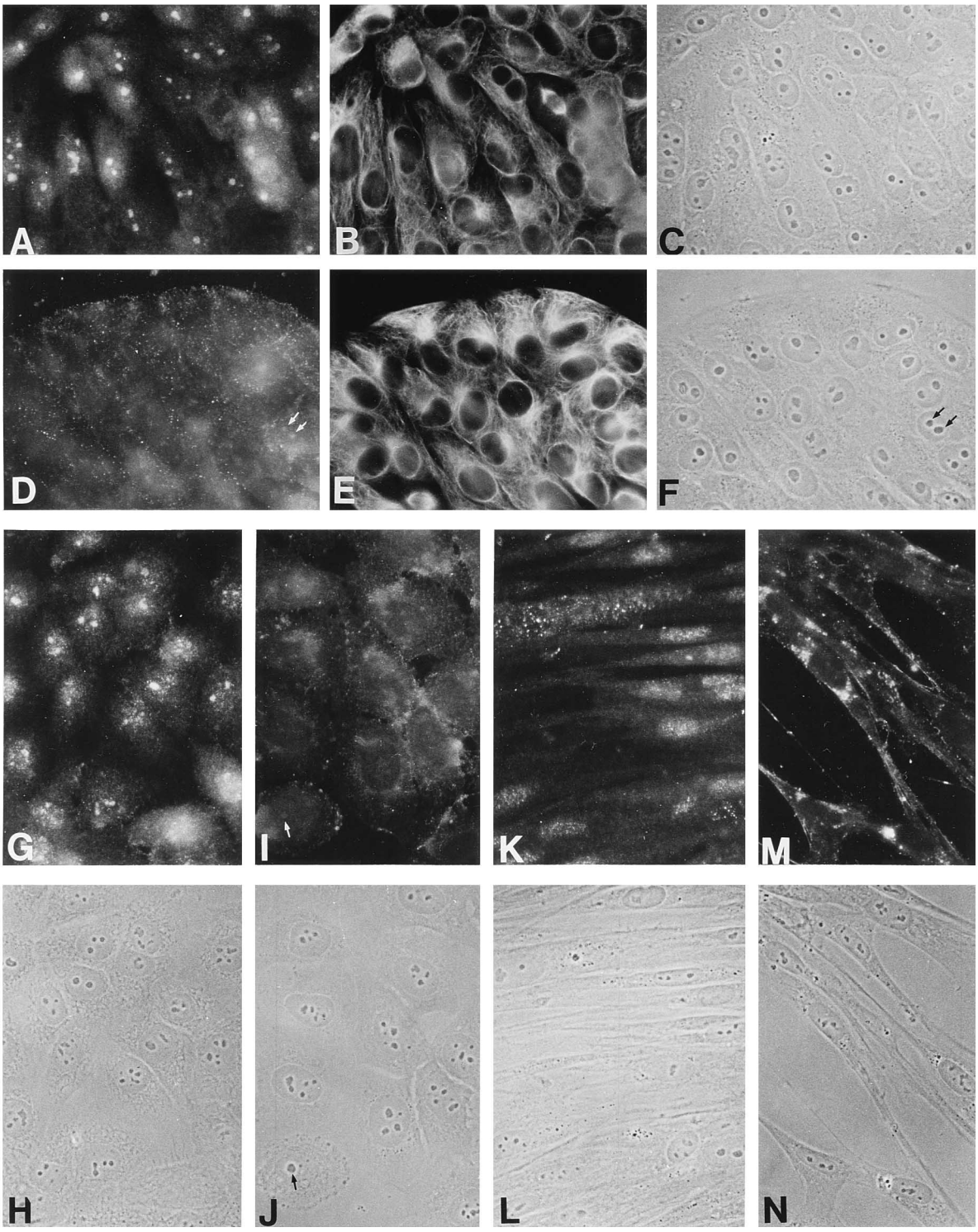

FIG. 6. Extinction of αp60 staining by preincubation with purified chicken c-Src in KHOS-240 (A to F), HeLa (G to J), and WI-38 (K to N) human cell lines. The cells were double-stained with anti-tubulin (B and E) and αp60 serum alone (A, G, and K) or αp60 serum preincubated with 7 μg of purified c-Src (D, I, M). (C and F and H, J, L, and N) Phase-contrast microscopy of cells shown in panels A to E and H, J, L, and N, respectively. The nuclear and nucleolar αp60 staining was almost totally extinguished in the presence of 7 μg of purified c-Src per ml, but the anti-tubulin labeling was not extinguished. Faint nucleolar labeling persisted in some cells at this c-Src concentration (D, F, I, and J, tiny arrows).

(GNS11) then allowed the correlation of possible changes in the immunolocalization patterns of the αp60-reactive protein with entry into the G_2 phase. The results of this experiment, depicted in Fig. 8, clearly indicate that cells exhibiting an increased level of extranucleolar αp60 staining also express a highly enhanced level of cytoplasmic cyclin B1 (Fig. 8, large arrows). It has also been documented previously with HeLa cells that at the beginning of prophase, before nuclear mem-

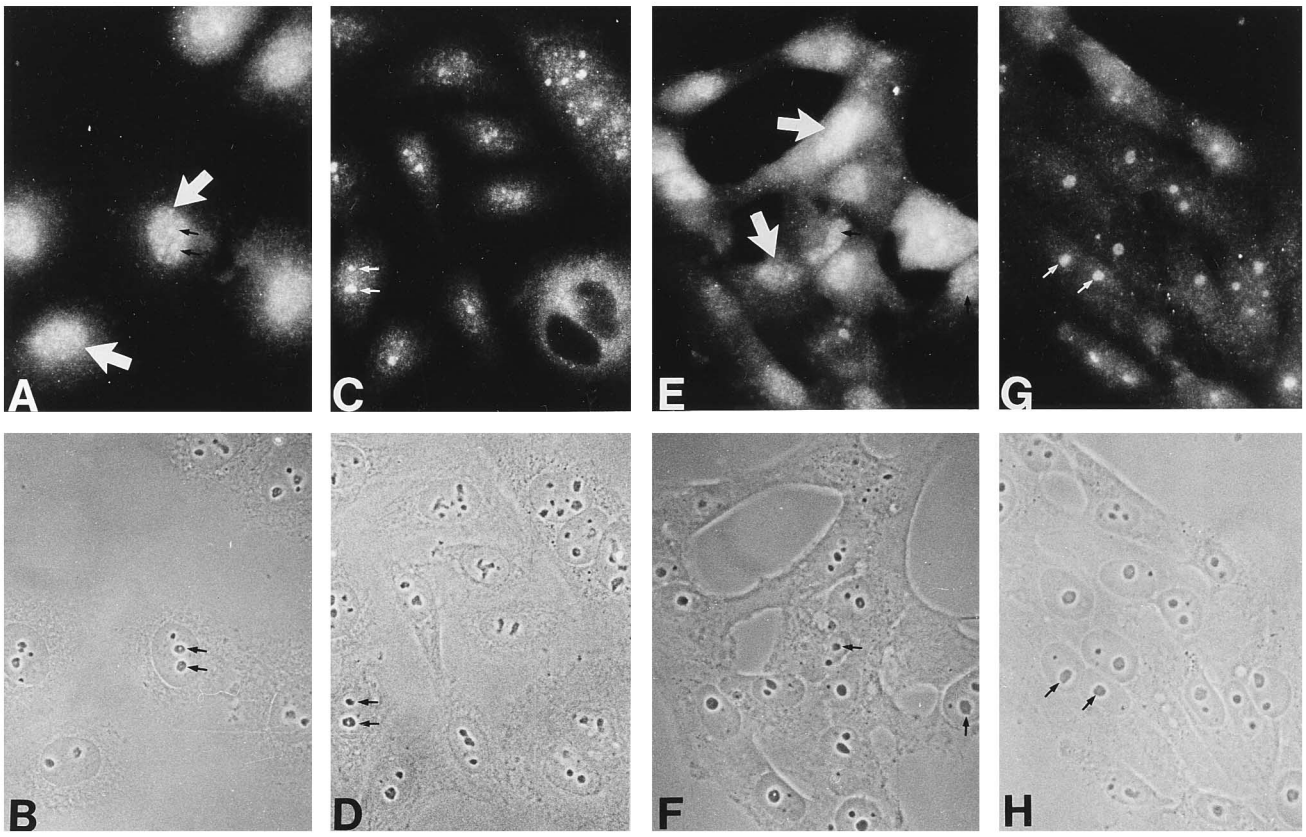

FIG. 7. Immunolabeling with αp60 serum (A, C, E, and G) and corresponding phase-contrast images (B, D, F, and H) of HeLa (A to D) and KHOS-240 (E to H) cells following release from thymidine-aphidicolin double block. (A and E) At time zero following double-block release, a majority of cells in the two cell lines exhibited strong αp60 nuclear staining (large arrows), including apparent staining of the nucleoli (tiny arrows). A few hours following double-block release (6 h in panels C and G) much of the nuclear αp60 staining had vanished, with reappearance of the major nucleolar labeling typical of interphase cells (tiny arrows).

brane breakdown, almost all the cytoplasmic pool of cyclin B1 is precipitously redistributed in the nucleus (38). It is generally at this stage that the highest levels of extranucleolar αp60-specific immunostaining are detected in both HeLa and KHOS-240 cells (Fig. 8, arrowheads). Cells undergoing a G_2-M transition can also be recognized by their typically punctate DAPI staining (Fig. 8N, arrowhead), which signals the beginning of chromosome condensation. At this stage, according to phase-contrast microscopy, the nuclei remain well defined and the nucleoli which can still be observed (Fig. 8L and O, tiny arrows) continue to exhibit bright αp60 immunostaining (Fig. 8M, tiny arrow). Later, as chromosomes keep rearranging but do not yet show a significant degree of condensation, and as the nuclear contours are no longer distinguishable by phase contrast microscopy (Fig. 9C and F, large arrowheads), the cyclin B1 staining still heavily concentrates in the previously nuclear space while the αp60 staining itself tends to totally vanish (Fig. 9A, B, D, and E, large arrowheads).

From prometaphase to early telophase, light αp60 immunostaining (Fig. 9G), diffusely distributed throughout the mitotic cells, persists whereas intense cyclin B1 staining persists to the metaphase (Fig. 9H). Both the faint αp60 staining and the strong cyclin B1 staining tend to avoid the condensed chromosomes (Fig. 9G, H, and I, tiny arrows). In late telophase and early postmitotic cells (Fig. 9G to I, two lower cells, and Fig. 9J to L, all cells) which remain connected through the midbody (Fig. 9L, black arrowheads), the cyclin B1 staining remains absent; in contrast, the αp60-associated fluorescence reappears very rapidly in late-telophase cells, first in association with the still-condensed chromosomes around which a nuclear membrane has apparently rebuilt (Fig. 9J to L, long arrows). But, as soon as the chromosomes begin to decondense, with the nuclei expanding and well-defined nucleoli reappearing, the preferential interaction between the αp60-reactive Src molecules and the nucleoli is restored (Fig. 9J and L, tiny arrows).

In contrast to the human tumor-derived cell lines, untransformed WI-38 could readily be blocked in G_0 phase following serum deprivation down to 0.5% for 3 days. Under these conditions indeed, less than 2% of the cells were found to have accumulated significant levels of nuclear cyclin A and very rarely was a mitotic cell encountered. Interestingly, however, with αp60 serum, the presence of an anti-$pp60^{src}$-reactive protein was still detected inside tiny dots spreading throughout the nucleus but seldom concentrated at an elevated level in the nucleoli. As the cells progressed through interphase, following serum stimulation, an enhancement in the intensity of nuclear αp60 immunostaining could not be clearly visualized. But, at the G_2-M transition, as the chromosomes were starting to appear well defined in phase contrast (Fig. 9O, large arrowhead) as well as with the DAPI staining (Fig. 9N, large arrowhead), the αp60-immunoreactive antigens clearly diffused out from the space occupied by the chromosomes (Fig. 9M, large arrowhead) and remained dispersed through the cytoplasm during the full mitosis (data not shown), as in the tumor-derived cell lines.

Changes in immunolocalization patterns of αp60-immuno-

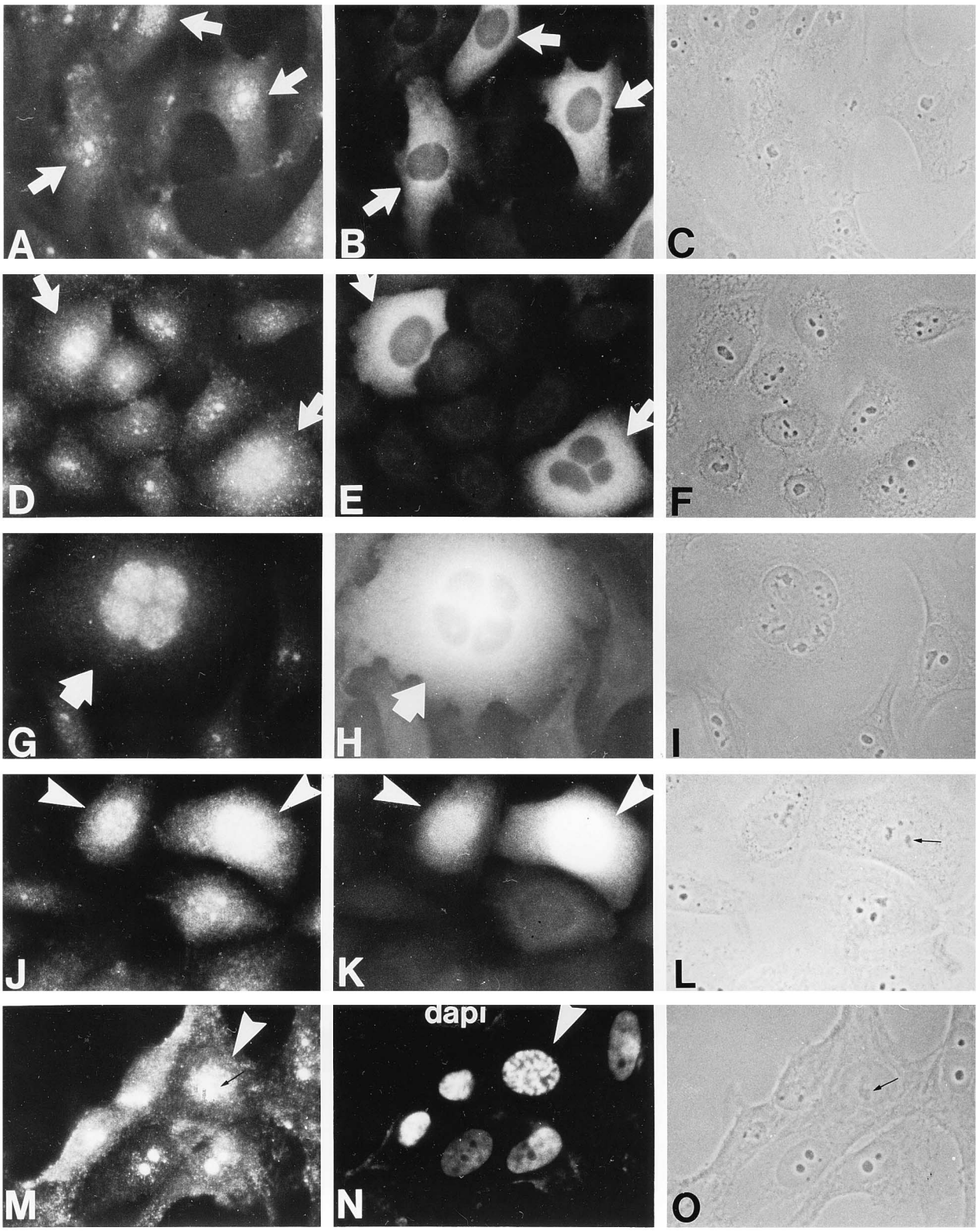

FIG. 8. Immunolocalization of αp60-reactive antigens as a function of the cell cycle in HeLa (D and J) and KHOS-240 (A, G, and M) cells prior G_2-M transition. The cells were doubly labeled with αp60 (A, D, G, J, and M) and anti-cyclin B1 (B, E, H, and K) or DAPI (N) (middle row). (C, F, I, and O) Phase-contrast images of the cell fields in the same horizontal rows. The large arrows point out G_2 cells that display abundant cytoplasmic accumulation of cyclin B1 and in which nuclear αp60 immunostaining was more abundant than in cyclin B1-negative cells.

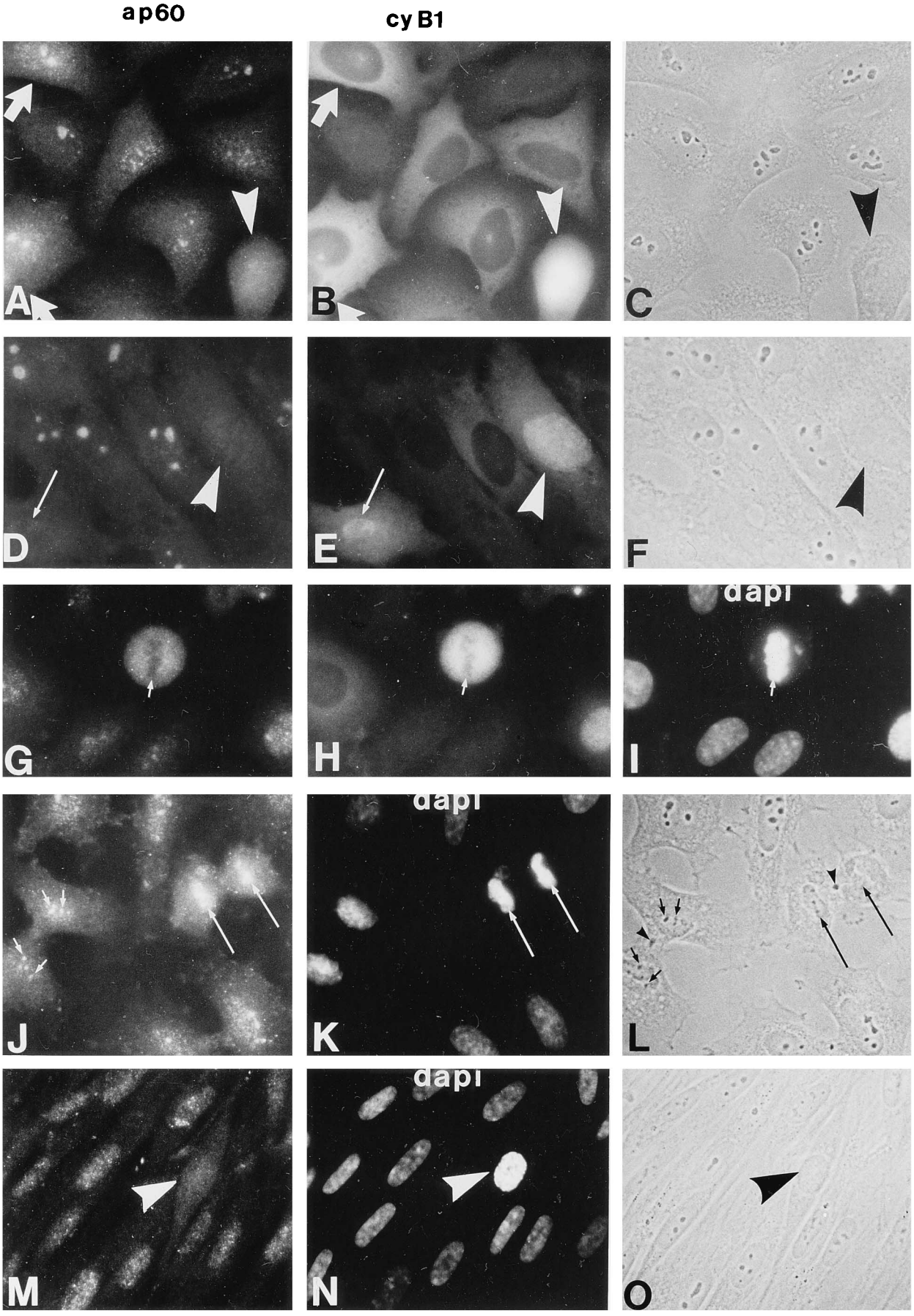

FIG. 9. Immunolocalization of αp60-reactive antigens during mitosis in HeLa (A, G, and J), KHOS-240 (D), and WI-38 (M). The cells were doubly labeled with αp60 (A, D, G, J, and M) and anti-cyclin B1 (B, E, and H) or DAPI (K and N) or triply labeled with αp60 (G), anti-cyclin B1 (H), and DAPI (I). (C, F, L, and O) Phase-contrast images of cell fields in the same horizontal rows.

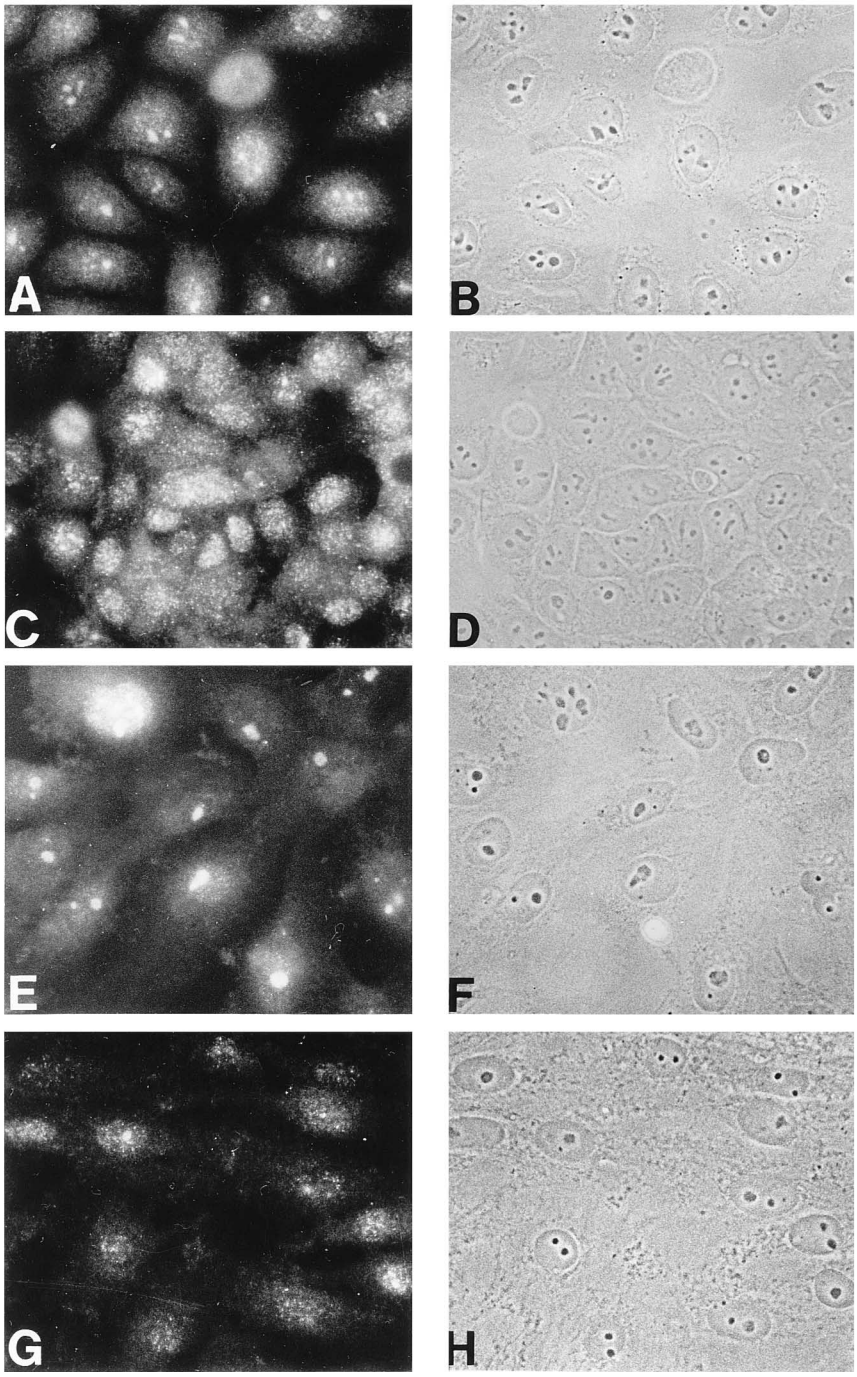

FIG. 10. Immunolocalization of αp60-reactive antigens as a function of cell density in HeLa (A to D) and KHOS-240 (E to H) cells. (B, D, F, H) Phase-contrast images of the cell fields in the same horizontal rows. In subconfluent cultures, the αp60 immunostaining resides predominantly in the nucleoli (A and E) whereas it becomes dispersed throughout the whole nuclear space at more elevated cell densities, as the cells touch each others (C and G).

reactive antigens as a function of cell-to-cell contact formation. In the tumor cell lines of the B group, it was noticeable that the cells situated at the periphery of the bidimensional multicellular aggregates preferentially exhibited the nucleolar αp60 immunostaining (Fig. 5E and F, tiny arrows), whereas the extranucleolar staining was augmented in the cells squeezed inside the aggregates (Fig. 5E and F, arrows). If such an effect resulted from the fact that these cells form strong intercellular contacts after cell divisions instead of dissociating and migrating apart on the glass or plastic substratum, then it was expected that the same phenomenon could possibly occur in HeLa and KHOS-240 cell populations reaching confluency. This is indeed what happens. In Fig. 10, different fields of HeLa (Fig. 10A to D) and KHOS-240 (Fig. 10E to H) cells that have reached different degrees of confluency are shown. Obviously, in subconfluent cultures, the αp60-reactive antigens reside predominantly in the nucleoli (Fig. 10A and E) whereas the extranuclear αp60 staining becomes more prominent at

more elevated cell densities (Fig. 10C and G). Such apparent redistribution at confluency of the αp60 immunostaining from mostly nucleolar to more dispersed throughout the whole nuclear space was observed as well following cell fixation with methanol at −20°C instead of with 3% paraformaldehyde at room temperature.

In the untransformed WI-38 cell line, the αp60-reactive antigens never appear to exhibit a preferential nucleolar association but rather tend to disperse into tiny dots throughout the whole nucleus at low, intermediate, and high cell densities (Fig. 5A).

DISCUSSION

This paper describes the detection, by indirect immunofluorescence microscopy, of nuclear and nucleolar subpopulations of an anti-pp60^{src}-reactive antigen in five human tumor-derived (KHOS-240, T47-D, A-431, MCF-7, and HeLa) cell lines and one untransformed (WI-38) cell line. This particular population of human protein is clearly revealed uniquely with αp60 serum, a polyclonal antibody raised in rabbits immunized with pp60$^{v\text{-}src}$ expressed in *E. coli* (41) but not with the most widely utilized mouse anti-Src MAb, 327 (27), or another anti-Src MAb, GD11 (37). For this reason we have named it the αp60-reactive antigen. Our immunoprecipitation experiments with αp60 serum indicate that the only additional band appearing above the background of proteins unspecifically retained on the protein A-Sepharose matrix, although faint, migrates at the same level as the 60-kDa proteins immunoprecipitated by MAbs 327 and GD11 acknowledged to be bona fide anti-Src antibodies. In spite of the fact that the immunolabeling of the human cells with MAb 327 and αp60, respectively, revealed immunoreactive proteins distributed in different subcellular compartments, in Western blots MAb 327 recognized the 60-kDa molecules specifically adsorbed by the αp60 antibodies. This finding supports the hypothesis that the 60-kDa protein immunoprecipitated by αp60 is indeed immunologically related to Src. The additional control experiment demonstrating that nuclear and nucleolar αp60 immunostaining could be totally extinguished by preincubation of the serum (dilution, 1:1,500) with 15 μg (0.25 μM) of a 95% pure c-Src preparation per ml further reinforces our confidence that we have identified αp60-reactive subpopulations of a human protein closely related to both pp60$^{v\text{-}src}$ (the antigen used to raise the antisera) and pp60$^{c\text{-}src}$ (the protein used in the extinction experiments). It should be recalled that the αp60 serum had been initially reported to recognize novel populations of pp60$^{v\text{-}src}$ and pp60$^{c\text{-}src}$ proteins copurifyed with nuclear fractions and undetected by tumor-bearing rabbit antisera in Schmidt-Ruppin strain Rous sarcoma virus-infected and uninfected chicken embryo fibroblasts. Therefore, the finding that this same serum is able to reveal very specifically in various human cell lines nuclear subpopulations of possible Src proteins which are undetectable with two different anti-Src MAbs should not be surprising. Furthermore, MAbs recognize a single epitope of the antigen against which they have been raised, in contrast to polyclonal antibodies which contain sets of IgG directed against multiple antigenic sites of the molecule. In consequence, if a protein assumes several conformational states in vivo, polyclonal antibodies are more likely than MAbs to uncover all of them. In addition, αp60 serum labels subcellular compartments which are labeled as well by the two anti-Src MAbs, in particular in embryonic, normal and transformed mouse and rat cells. This indicates that the αp60 serum contains some sets of IgG which react with pp60$^{c\text{-}src}$ and pp60$^{v\text{-}src}$ populations that are also recognized by MAb327 and GD11. Noticeably, the relative partitioning of the αp60 immunolabeling among the whole nucleus and the nucleolus in human cells was not random but appeared to depend mainly on two different parameters: (i) the position in the cell cycle and (ii) the extent of cell-to-cell aggregation. These observations argue against the possibility of an artefactual, unspecific interaction between the αp60 antibodies and nuclear structures. Finally our finding of a nuclear anti-pp60^{src}-reactive protein population in various tumor cell lines derived from adult tissues which still have the capacity to express some characteristics of the differentiated state was a possibility on the basis of the report by Zhao et al. (47) that c-Src is apparently able to translocate into the nucleus in response to in vitro calcium-induced keratinocyte differentiation. Interestingly, a similar nuclear αp60-reactive antigen has also been detected in three hepatoma cell lines derived from adult human, rat, and mouse tumors, whereas we failed to detect it in any continuous rat and mouse cell lines (Rat1, FR3T3, and NIH 3T3, all of which are derived from embryonic tissues), either untransformed or transformed by the *src* or *ras* oncogene. It is then remarkable that this nuclear anti-pp60^{src}-reactive protein is readily seen in the WI-38 human cell line derived from normal embryonic (3-month gestation) lung tissue.

In exponentially growing cell populations, the αp60 immunostaining partitionates among two different nuclear compartments: (i) the nucleolus, where it generally is concentrated the most heavily, and (ii) the extranucleolar space, where it is condensed inside tiny homogeneously scattered dots. In cells from the group of tumorous cell lines whose cells remain well dispersed on the plates (KHOS-240 and HeLa), nucleolar staining prevails over extranucleolar staining during the interphase, except in G_2 in which this predominance greatly diminishes and occasionally inverts. The most prominent nuclear αp60 staining is currently observed in cells entering prophase at the precise time when the cytoplasmic pool of cyclin B1 massively translocates inside the nucleus (38), after which the αp60-reactive antigens appear to be suddenly chased away from the nuclear space. This event, however, occurs very early in the prophase when cyclin B1 itself, to this time, continues to concentrate heavily in this location. Finally, the αp60-reactive antigens recover their preferential nuclear distribution very fast after the two daughter cells have become well individualized, even before the chromosomal material has begun to decondense significantly, and nucleolar segregation occurs again as soon as well-defined nucleoli have reformed.

Enzyme-substrate reactions require not only the presence of stereospecific sites of interaction but also a high probability of collision between the two molecules. In test tubes, the second condition can readily be satisfied by bringing together sufficient concentrations of enzyme and substrate in solution, often at concentrations higher than the physiological concentrations that seem to be available in the cell. That is why triggering an enzymatic reaction in vivo might necessitate the targetting of both enzyme and substrate inside the same subcellular compartment where they would achieve local concentrations exceeding the threshold levels needed to initiate the reaction. On the contrary, sequestrating an enzyme and its potential substrates in different subcellular compartments might be one way to prevent unscheduled enzymatic reactions. Then, one expects that the human αp60-reactive antigens will not interact with the same targets in the nucleolus and in the extranucleolar space within the nucleus. It is tempting to speculate that human p34^{cdc2}, which in mammalian cells has been located in part within the nucleus (1, 3, 43), could serve as a physiological substrate for the tyrosine kinase activity of a possible nuclear subset of Src proteins, considering two previous reports that p34^{cdc2} could be phosphorylated on tyrosine residues by using

baculovirus-expressed pp60$^{c\text{-}src}$ (15, 16). Two other groups, however, have failed to observe in vitro phosphorylation by purified c-Src proteins of human p34^{cdc2} (30) or of its homolog purified from metaphase-arrested *Xenopus* eggs (45). These divergences could possibly result from differences in the experimental conditions. Indeed, since Cdc2 would be active as kinase only when tyrosine dephosphorylated (for a review, see reference 33), we would expect that Cdc2 would be capable of phosphorylating c-Src only under conditions in which the initial rate of phosphorylation of Cdc2 by c-Src is lower than the initial rate of reciprocal phosphorylation of c-Src by Cdc2. This may explain why the investigators also failed to observe in vitro activation of the kinase activity of purified pp60$^{c\text{-}src}$ following p34^{cdc2}-induced hyperphosphorylation.

The observation that the treatment of human tumor cells with DNA synthesis inhibitors (thymidine and aphidicolin) results in a significant redistribution of the αp60-reactive molecules throughout the whole nuclear space may be of interest considering the other observation that this treatment induces a concomitant and dramatic accumulation of the tyrosine-phosphorylated form of the p34^{cdc2} kinase in these same cells (13a) as it does in sea urchin eggs (29) and BHK21 cells (32). At last, it is also noticeable that nucleolar αp60-specific immunostaining tends to diminish, whereas extranucleolar staining remains and even increases as the cells begin to touch and form intercellular contacts. It is well-known that cultured cells generally exhibit contact inhibition of growth at high cell densities. Cell cycle arrest at confluency may involve, in part, changes in the nuclear location of cell cycle regulatory proteins. This dependency of the cell cycle on intercellular contacts and/or the cell-to-cell contact structures themselves is greatly impaired in transformed cells which grow to higher cell densities than normal cells in culture, eventually piling up and acquiring the capacity to grow in semisolid medium or even in suspension (for a review, see reference 34). Now, distinctive subcellular populations of pp60$^{c\text{-}src}$ and related proteins have been uncovered, at both extremities of this regulatory pathway which connects plasma membrane-associated events (that signals either mitogenic stimulation or growth inhibition by cell-to-cell contact formation) to the cell cycle engine, which operates mainly in the nucleus around its most critical components, the p34^{cdc2} and the Cdc2-related protein kinases. Therefore, it is likely that pp60$^{c\text{-}src}$ and members of its family are major elements of this regulatory pathway which subjects the cell cycle engine to the control of the cellular environment and whose alteration is necessary for the generation of cancer.

ACKNOWLEDGMENTS

We express special thanks to Marylin Resh for her generous and precious gift of the αp60 antisera upon which this work essentially relies. We are also grateful to Sarah Parsons, Steven Shiff, and Ed Harlow and Mossaad Abdel-Ghany, Ben Hilton, and David Shalloway, who kindly provided anti-Src and anti-cyclin B1 antibodies and purified chicken c-Src, respectively. We also acknowledge Irène Gaspard and Didier Auffret for expert artwork and Madame Françoise Arnouilh for typing the manuscript.

This study was supported by the Centre National pour la Recherche Scientifique, the Curie Institute, and the Association pour la Recherche sur le Cancer.

REFERENCES

1. **Akhurst, R. J., N. B. Flavin, J. Worden, and M. G. Lee.** 1989. Intracellular localisation and expression of mammalian cdc2 protein during myogenic differentiation. Differentiation **40:**36–41.
2. **Bagrodia, S., I. Chackalaparampil, T. E. Kmiecik, and D. Shalloway.** 1991. Altered tyrosine 527 phosphorylation and mitotic activation of p60^{src}. Nature (London) **349:**172–175.
3. **Bailly, E., M. Dorée, P. Nurse, and M. Bornens.** 1989. p34^{cdc2} is located in both nucleus and cytoplasm; part is centrosomally associated at G2/M and enters vesicles at anaphase. EMBO J. **8:**3985–3995.
4. **Bailly, E., J. Pines, T. Hunter, and M. Bornens.** 1992. Cytoplasmic accumulation of cyclin B1 in human cells: association with a detergent-resistant compartment and with the centrosome. J. Cell Sci. **101:**529–545.
5. **Barnekow, A., J. Reinhard, and M. Schartl.** 1990. Synaptophysin: substrate for the protein tyrosine kinase pp60$^{c\text{-}src}$ in intact synaptic vesicles. Oncogene **5:**1019–1024.
6. **Barnekow, A., and M. Schartl.** 1984. Cellular *src* gene product detected in the freshwater sponge *Spongilla lacustris*. Mol. Cell. Biol. **4:**1179–1181.
7. **Bartek, J., R. Iggo, J. Gannon, and D. P. Lane.** 1990. Genetic and immunochemical analysis of mutant p53 in human breast cancer cell lines. Oncogene **5:**893–899.
8. **Chackalaparampil, I., and D. Shalloway.** 1988. Altered phosphorylation and activation of pp60$^{c\text{-}src}$ during fibroblast mitosis. Cell **52:**801–810.
9. **Chen, P. L., Y. Chen, R. Bookstein, and W. H. Lee.** 1990. Genetic mechanisms of tumor suppression by the human p53 gene. Science **250:**1576–1579.
10. **Cooper, J. A.** 1990. The Src family of protein tyrosine kinases, p. 85–113. *In* B. Kamp and P. F. Alewood (ed), Peptide and protein phosphorylations. CRC Press, Inc., Boca Raton, Fla.
11. **Cotton, P. C., and J. S. Brugge.** 1983. Neural tissues express high levels of the cellular *src* gene product pp60$^{c\text{-}src}$. Mol. Cell. Biol. **3:**1157–1162.
12. **David-Pfeuty, T., S. Bagrodia, and D. Shalloway.** 1993. Differential localization patterns of myristoylated and nonmyristoylated c-Src proteins in interphase and mitotic c-Src overexpresser cells. J. Cell Sci. **105:**613–628.
13. **David-Pfeuty, T., and Y. Nouvian-Dooghe.** 1990. Immunolocalization of the cellular src protein in interphase and mitotic NIH c-src overexpresser cells. J. Cell Biol. **111:**3097–3116.

13a. **David-Pfeuty, T., and Y. Nouvian-Dooghe.** Unpublished results.

14. **David-Pfeuty, T., and J. S. Singer.** 1980. Altered distributions of the cytoskeletal proteins vinculin and α-actinin in cultured fibroblasts transformed by Rous sarcoma virus. Proc. Natl. Acad. Sci. USA **77:**6687–6691.
15. **Draetta, G., and D. Beach.** 1988. Activation of cdc2 protein kinase during mitosis in human cells: cell cycle-dependent phosphorylation and subunit rearrangement. Cell **54:**17–26.
16. **Gautier, J., M. J. Solomon, R. N. Booher, J. F. Bazan, and M. W. Kirschner.** 1991. cdc25 is a specific tyrosine phosphatase that directly activates p34^{cdc2}. Cell **67:**197–211.
17. **Gilmer, T. M., and R. L. Erickson.** 1983. Development of anti-pp60^{src} serum with antigen produced in *Escherichia coli*. J. Virol. **45:**462–465.
18. **Girard, F., U. Strausfeld, A. Fernandez, and N. J. C. Lamb.** 1991. Cyclin A is required for the onset of DNA replication in mammalian fibroblasts. Cell **67:**1169–1179.
19. **Goddard, C., S. T. Arnold, and R. L. Felsted.** 1989. High affinity binding of an N-terminal myristoylated p60^{src} peptide. J. Biol. Chem. **264:**15173–15176.
20. **Golden, A., S. P. Nemeth, and J. S. Brugge.** 1986. Blood platelets express high levels of pp60$^{c\text{-}src}$ specific tyrosine kinase activity. Proc. Natl. Acad. Sci. USA **83:**852–856.
21. **Grandori, C., and H. Hanafusa.** 1988. pp60$^{c\text{-}src}$ is complexed with a cellular protein in subcellular compartment involved in exocytosis. J. Cell Biol. **107:**2125–2135.
22. **Johnson, P. J., P. M. Coussens, A. V. Danko, and D. Shalloway.** 1985. Overexpressed pp60$^{c\text{-}src}$ can induce focus fomration without complete transformation of NIH 3T3 cells. Mol. Cell. Biol. **5:**1073–1083.
23. **Jove, R., and H. Hanafusa.** 1987. Cell transformation by the viral src oncogene. Annu. Rev. Cell. Biol. **3:**31–56.
24. **Kaech, S., L. Covic, A. Wyss, and K. Ballmer-Hofer.** 1991. Association of pp60$^{c\text{-}src}$ with polyoma virus middle-T abrogates mitosis-specific activation. Nature (London) **350:**431–433.
25. **Kaplan, K. B., J. R. Swedlow, H. E. Varmus, and D. O. Morgan.** 1992. Association of pp60$^{c\text{-}src}$ with endosomal membranes in mammalian fibroblasts. J. Cell Biol. **118:**321–333.
26. **Linstedt, A. D., M. L. Vetter, J. M. Bishop, and R. B. Kelly.** 1992. Specific association of the proto-oncogene product pp60$^{c\text{-}src}$ with an intracellular organelle, the PC12 synaptic vesicle. J. Cell Biol. **177:**1077–1084.
27. **Lipsich, L. A., A. J. Lewis, and J. S. Brugge.** 1983. Isolation of monoclonal antibodies that recognize the transforming protein of avian sarcoma viruses. J. Virol. **48:**352–360.
28. **May, E., J. R. Jenkins, and P. May.** 1991. Endogenous HeLa p53 proteins are easily detected in HeLa cells transfected with mouse deletion mutant p53 gene. Oncogene **6:**1363–1365.
29. **Meijer, L., Azzi, L., and J. Y. J. Wang.** 1991. Cyclin B targets p34^{cdc2} for tyrosine phosphorylation. EMBO J. **10:**1545–1554.
30. **Morgan, D. O., J. M. Kaplan, J. M. Bishop, and H. E. Varmus.** 1989. Mitosis-specific phosphorylation of pp60$^{c\text{-}src}$ by p34^{cdc2}-associated protein kinase. Cell **57:**775–786.
31. **Nigro, J. M., S. J. Baker, A. C. Preisinger, J. M. Jessup, R. Hostetter, K. Cleary, S. H. Bigner, N. Davidson, S. Baylin, P. Devilee, T. Glover, F. S. Collins, A. Weston, R. Modali, C. C. Harris, and B. Vogelstein.** 1989. Mutations in the p53 gene occur in diverse human tumour types. Nature (London) **342:**705–708.
32. **Nishitani, H., Ohtsubo, M., Yamashita, K., Pines, J., Yasudo, H., Shibata,**

Y., Hunter, T., and T. Nishimoto. 1991. Loss of RCCC1, a nuclear DNA-binding protein, uncouples the completion of DNA replication from the activation of cdc2 protein kinase and mitosis. EMBO J. **10:**1555–1564.
33. **Nurse, P.** 1990. Universal control mechanism regulating the onset of M-phase. Nature (London) **344:**503–508.
34. **Pardee, A. B.,** 1989. G_1 events and regulation of cell proliferation. Science **246:**603–608.
35. **Parsons, J. T., and M. J. Weber.** 1989. Genetic of src: structure and functional organization of a protein tyrosine kinase. Curr. Top. Microbiol. Immunol. **147:**79–127.
36. **Parsons, S. J., and C. E. Creutz.** 1986. $pp60^{c\text{-}src}$ activity detected in the chromaffin granule membrane. Biochem. Biophys. Res. Commun. **134:**736–742.
37. **Parsons, S. J., D. J. McCarley, C. M. Ely, D. C. Benjamin, and J. T. Parsons.** 1984. Monoclonal antibodies to Rous sarcoma virus $pp60^{src}$ react with enzymatically active $pp60^{src}$ of avian and mammalian origin. J. Virol. **51:**272–282.
38. **Pines, J., and T. Hunter.** 1991. Human cyclin A and B1 are differentially located in the cell and undergo cell cycle-dependent nuclear transport. J. Cell Biol. **115:**1–17.
39. **Rendu, F., M. Lebret, S. Danielen, R. Fagard, S. Levy-Toledano, and S. Fisher.** 1989. High $pp60^{c\text{-}src}$ level in human platelet dense bodies. Blood **73:**1545–1551.
40. **Resh, M. D.** 1989. Specific and saturable binding of $pp60^{v\text{-}src}$ to plasma membranes: evidence for a myristyl-src receptor. Cell **58:**281–286.
41. **Resh, M. D., and R. L. Erikson.** 1985. Highly specific antibody to Rous sarcoma virus src gene product recognize a novel population of $pp60^{v\text{-}src}$ and $pp60^{c\text{-}src}$ molecules. J. Cell Biol. **100:**409–417.
42. **Resh, M. D., and H. Ling.** 1990. Identification of a 32 K plasma membrane protein that binds to the myristylated amino terminal sequence of $pp60^{v\text{-}src}$. Nature (London) **346:**84–86.
43. **Riabowol, K., G. Draetta, L. Brizuela, D. Vandre, and D. Beach.** 1989. The cdc2 kinase is a nuclear protein that is essential for mitosis in mammalian cells. Cell **57:**393–401.
44. **Romano, J. W., J. C. Ehrhart, A. Duthu, C. M. Kim, E. Appella, and P. May.** 1989. Identification and characterization of a p53 gene mutation in a human osteosarcoma cell line. Oncogene **4:**1483–1488.
45. **Shenoy, S. J., J. K. Choi, S. Bagrodia, T. D. Copeland, J. L. Maller, and D. Shalloway.** 1989. Purified maturation promoting factor phosphorylates $pp60^{c\text{-}src}$ at the sites phosphorylated during fibroblast mitosis. Cell **57:**763–774.
46. **Spector, D. H., H. E. Varmus, and J. M. Bishop.** 1978. Nucleotide sequences related to the transforming gene of avian sarcoma virus are present in DNA of uninfected vertebrates. Proc. Natl. Acad. Sci. USA **9:**4102–4106.
47. **Zhao, Y., M. Sudol, H. Hanafusa, and I. Krueger.** 1992. Increased tyrosine kinase activity of c-Src during calcium-induced keratinocyte differentiation. Proc. Natl. Acad. Sci. USA **89:**8298–8302.
48. **Zhang, S., K. El-Gendy, M. Abdel-Ghany, R. Clark, F. McCormick, and E. Racker.** 1991. Isolation of highly purified and stable preparations of c-src and v-src kinase. Cell. Physiol. Biochem. **1:**24–30.